Mon. Not. R. Astron. Soc. **000**, 1–6 (2012) Printed 12 April 2013 (MN LATEX style file v2.2)

Powering of cool filaments in cluster cores by buoyant bubbles. I. Qualitative model.

E. Churazov[1,2], M. Ruszkowski[3,4], A. Schekochihin[5]
[1] *MPI für Astrophysik, Karl-Schwarzschild str. 1, Garching, 85741, Germany*
[2] *Space Research Institute, Profsoyuznaya str. 84/32, Moscow, 117997, Russia*
[3] *Department of Astronomy, The University of Michigan, 500 Church Street, Ann Arbor, MI 48109, USA*
[4] *The Michigan Center for Theoretical Physics, 3444 Randall Lab, 450 Church St, Ann Arbor, MI 48109, USA*
[5] *The Rudolf Peierls Center for Theoretical Physics, University of Oxford, 1 Keble Road, Oxford, OX1 3NP, UK*

Accepted .... Received ...

ABSTRACT

Cool-core clusters (e.g., Perseus or M87) often possess a network of bright gaseous filaments, observed in radio, IR, optical and X-ray bands. We propose that these filaments are powered by the reconnection of the magnetic field in the wakes of buoyant bubbles. AGN-inflated bubbles of relativistic plasma rise buoyantly in the cluster atmosphere, stretching and amplifying the field in the wake to values of $\beta = 8\pi P_{gas}/B^2 \sim 1$. The field lines in the wake have opposite directions and are forced together as the bubble motion stretches the filament. This setup bears strong similarity to the coronal loops on the Sun or the Earth magneto-tail. The reconnection process naturally explains both the required level of local dissipation rate in filaments and the overall luminosity of filaments. The original source of power for the filaments is the potential energy of buoyant bubbles, inflated by the central AGN.

Key words: methods: numerical - galaxies: clusters: intracluster medium - X-rays: galaxies: clusters

1 INTRODUCTION

Networks of bright gaseous filaments are ubiquitous in the centers of cool-core clusters (e.g., McDonald et al. 2010). H_α filaments around NGC1275 in the Perseus cluster are perhaps the most famous example (e.g., Minkowski 1957; Lynds 1970). These filaments are observed in many bands/lines, including CO (e.g., Lazareff et al. 1989; Salomé et al. 2006), NIR lines (Mittal et al. 2012), optical lines (e.g., Conselice, Gallagher, & Wyse 2001) and soft X-rays (Fabian et al. 2003), suggesting a multi-temperature gas sharing approximately the same space within the cluster. For a recent summary of observational results on NGC1275 and M87 filaments see, e.g., Fabian et al. (2011); Werner et al. (2012) and references therein. Below we discuss NGC1275 and M87 collectively, under implicit assumption that the same mechanism is responsible for the filamentary structures in both objects (and also in other cool-core clusters).

The source of energy powering the filaments is a long-standing problem. The bolometric luminosity of the filaments in the NIR-optical band could be at the level of 10-20% of the total X-ray luminosity of the cluster core. Various scenarios have been considered, including shocks (David, Bregman, & Seab 1988), photoionization by optical/UV or X-ray radiation (e.g., Heckman et al. 1989; Voit, Donahue, & Slavin 1994), thermal conduction (e.g., Boehringer & Fabian 1989). Ferland et al. (2009) argued that the spectra of the outer filaments require the line excitation by energetic particles, although not all line ratios are consistent with this scenario (Mittal et al. 2012). Recently Fabian et al. (2011) and Werner et al. (2012) suggested that the filaments are powered by the hot ICM, which penetrates into the filaments via turbulent reconnection.

The filaments are long and thin, probably consisting of many threads (Forman et al. 2007; Fabian et al. 2008). This suggests that the magnetic field is playing a role. The role of magnetic fields and in particular reconnection as a source of energy for filaments has been considered in, e.g., Soker & Sarazin (1990) and Jafelice & Friaca (1996). It was assumed that an inflow of cooling gas (in the frame of original cooling flow model) increases the magnetic energy density in the core of the cluster. The relative contribution of the magnetic field to the energy density is further amplified by the radiative cooling losses of the gas thermal energy.

Here we consider a different scenario, in which buoyant bubbles of relativistic plasma stretch the magnetic field lines

and drive the fields of opposite direction together. In this model the AGN-inflated bubbles provide the energy that powers the filaments. A schematic picture of this process is shown in Fig. 1.

The structure of this paper is as follows. In §2 we briefly summarize the relevant properties of AGN-inflated bubbles. In §3 we discuss the amplification of the magnetic field by the rising bubbles. In §4 we provide an order-of-magnitude estimate of the rate of energy dissipation by reconnecting magnetic fields in the bubble's tail and the resulting luminosity of the filaments. In §5 we discuss the overall energetics of filaments and the most basic properties of our model. Our findings are summarized in §6.

2 BUOYANT BUBBLES

Observations suggest that AGN activity regulates the thermal state of the gas by injecting energy into the intra-cluster medium in the cores of relaxed clusters, where radiative cooling time is often as short as few 10^8 years. Bubbles of relativistic plasma are inflated by a supermassive black hole and rise buoyantly through the gaseous atmosphere, leading to a number of spectacular phenomena such as expanding shocks, X-ray-dim and radio-bright cavities, X-ray-dim and radio-dim "ghost" cavities (aged versions of "normal" cavities) and filaments of cool gas in the wakes of the rising bubbles formed by the entrained low-entropy material from the core (Churazov et al. 2000, 2001). With Chandra and XMM-Newton, these features are now studied in great detail in many systems.

Observations further suggest that large fraction of energy output of the AGN goes into the enthalpy of the bubbles $H = \gamma_b P V_b/(\gamma_b - 1)$, rather than into shocks. Here γ_b is the adiabatic index of the gas inside the bubble ($\gamma_b = 4/3$ or $5/3$ depending on whether a relativistic or a non-relativistic gas is considered), P is the pressure inside the bubble and V_b is the bubble volume. The partitioning of the AGN energy between shocks and bubble enthalpy depends on the energy injection rate, duration of the AGN outburst and initial conditions (e.g., Forman et al. 2007, 2013), but fiducial models predict that about 70% (and certainly more than 50%) goes into the enthalpy of bubbles. Furthermore, the lack of very strong shocks around observed bubbles suggests that the thermal gas pressure of the ICM supporting the bubble, can be used in the above expression for the enthalpy H (i.e., $P \approx P_{gas}$, the bubble and the ICM are in pressure balance).

The bubbles then serve as a reservoir of potential of energy $\sim H$, deposited by the AGN. The dynamics of the bubble rise is set by the competition of the buoyancy force and the drag from the ambient gas. Even if we consider only the hydrodynamic drag (i.e., ignoring a possible contribution of magnetic fields) the rise velocity is expected to be subsonic (Churazov et al. 2000). Indeed, the buoyancy force is $F_b \sim \rho V_b g$, where g is the gravitational acceleration, and it is balanced by the ram pressure of the ICM (inertial drag force) $F_{ram} \sim A\rho v_{term}^2$, where v_{term} is the bubble's terminal velocity, A is the cross section of the bubble. Equating F_{ram} and F_b gives an expression of the terminal velocity $v_{term} \sim \sqrt{gR}$, where R is the bubble radius. The terminal velocity should be subsonic/transsonic as long as the bubble radius does not exceed the pressure scale height of the atmosphere. Assuming that the bubble is moving subsonically and does not mix with the ambient ICM, the volume of the bubble expands adiabatically $V_b = V_{b,0}\left(\frac{P}{P_0}\right)^{-\frac{1}{\gamma_b}}$, where $P = P(r)$, $P_0 = P(r_0)$ is the ICM pressure and r_0 and r are the initial and current distance of the bubble from the cluster center. For simplicity, we assume below a power-law dependence of pressure on the radius $P = P_0\left(\frac{r}{r_0}\right)^{-\alpha}$. Typically $\alpha \sim 0.7 - 1$ for the relevant range of radii in cool core clusters. For example, using radial density and temperature profiles from Churazov et al. (2003) and (Forman et al. 2007) we obtained $\alpha = 0.8$ and 0.9 for the Perseus cluster and M87 respectively.

The ambient material and the bubble itself can be threaded by the magnetic fields. As the bubble rises, the magnetic field is amplified – this process is discussed in the next section.

3 RISE OF THE BUBBLE

The role of magnetic fields in the evolution of buoyant bubbles has been considered in, e.g., Ruszkowski et al. (2007, 2008); O'Neill, De Young, & Jones (2009). Here we concentrate specifically on the threads of the magnetic field in the wake of a rising bubble.

A sketch of the configuration is shown in Fig.1. We assume that the bubble advects a lump of the ICM threaded by magnetic field lines, which are anchored to the gas in the cluster core. We assume that initially the reconnection of the magnetic field can be neglected. As the bubbles rise, the advected fluid elements and the magnetic field frozen into them are stretched by the bubble motion. We start by considering the evolution of such an advected fluid element occupying a volume $V \lesssim V_b$. As the fluid element moves from r_0 to r, its volume expands adiabatically $V = V_0\left(\frac{P}{P_0}\right)^{-\frac{1}{\gamma}}$, where γ is the adiabatic index of the ICM. The linear size of the stretched fluid element along the direction of motion can be estimated as $l \approx R_0 + r - r_0$, where R_0 is the initial size of the fluid element. In the limit $r \gg r_0$, $l \sim r$. The cross section A of the fluid element in the perpendicular direction is then

$$A \sim \frac{V}{l} \sim \frac{V_0}{l}\left(\frac{P}{P_0}\right)^{-\frac{1}{\gamma}} \sim \frac{V_0}{r}\left(\frac{r}{r_0}\right)^{\frac{\alpha}{\gamma}} \propto r^{\frac{\alpha}{\gamma}-1}. \quad (1)$$

Thus, for $\alpha < \gamma$, the cross section of the fluid element shrinks as the bubble rises.

The stretching of the fluid element will align and amplify the magnetic field B. From the conservation of the magnetic flux through the cross section of the advected fluid element:

$$\frac{B}{B_0} \sim \frac{A_0}{A} \sim \frac{l}{R_0}\left(\frac{P}{P_0}\right)^{\frac{1}{\gamma}} \sim \frac{r}{R_0}\left(\frac{r}{r_0}\right)^{-\frac{\alpha}{\gamma}}, \quad (2)$$

where B_0 is the initial magnetic field and $A_0 \sim V_0/R_0$ the

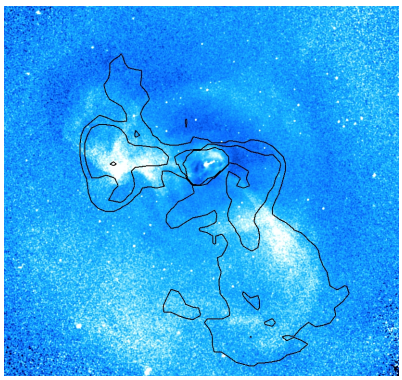

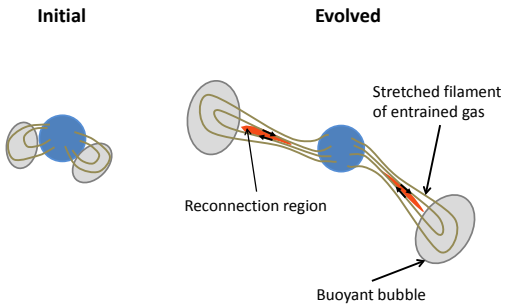

Figure 1. Qualitative picture of the current sheets formation by AGN-inflated buoyant bubbles of relativistic plasma, rising in the cluster atmosphere. Nearby elliptical galaxy M87/Virgo is used in this example. **Left:** Morphology of soft X-ray filaments in M87 (Forman et al. 2007) and overall morphology of the radio emitting plasma (Owen, Eilek, & Kassim 2000), superposed as contours. Optical filaments are largely co-spatial with X-ray filaments. Buoyant bubbles rise in the atmosphere, entraining the low entropy gas from the core (Churazov et al. 2000, 2001) and stretching/squeezing the fluid elements in the wake. Radio emission traces the distribution of the relativistic plasma produced by the AGN. **Right:** Schematic evolution of the magnetic field in the wake. As the bubbles rise they stretch the magnetic field lines in the entrained fluid elements, thus increasing the strength of the field. The field lines, anchored to the gas in the cluster core, have opposite directions in the wake. They are forced together as the bubble rises. This setup bears strong similarity to the coronal loops on the Sun or the Earth magneto-tail, where reconnection is taking place.

initial cross-section. The corresponding magnetic energy is

$$E_B = \frac{B^2}{8\pi}V = \frac{B_0^2}{8\pi}V_0\frac{l^2}{R_0^2}\left(\frac{P}{P_0}\right)^{\frac{1}{\gamma}} \sim \frac{P_0V_0}{\beta_0}\frac{r^2}{R_0^2}\left(\frac{r}{r_0}\right)^{-\frac{\alpha}{\gamma}}, \quad (3)$$

where $\beta_0 = 8\pi\dfrac{P_0}{B_0^2} \sim 100$ (e.g., Carilli & Taylor 2002) is the β parameter of the ICM near the initial position of the bubble. Using this expression, we can estimate the maximum distance r_{max} from the cluster center the bubble can reach – this is the radius where the buoyancy force $F_b \sim \rho V_b g \sim V_b\dfrac{dP}{dr} \sim V_b\dfrac{P}{r}$ is equal to $F_L \sim \dfrac{dE_B}{dr} \sim \dfrac{E_B}{r}$. In the limit of $r_{max} \gg r_0, R_0$, the equality $F_b \sim F_L$ is reached at

$$r_{max} \sim r_0\left(\beta_0\frac{V_{b,0}}{V_0}\frac{R_0^2}{r_0^2}\right)^{\frac{1}{2+\alpha-\alpha/\gamma-\alpha/\gamma_b}}. \quad (4)$$

At this radius, the value of β in the stretched fluid element is

$$\beta(r_{max}) \sim \frac{PV}{E_B} \sim \beta_0\frac{R_0^2}{r_0^2}\left(\beta_0\frac{V_{b,0}}{V_0}\frac{R_0^2}{r_0^2}\right)^{-\frac{2\gamma+\alpha(\gamma-2)}{2\gamma+\alpha(\gamma-1-\gamma/\gamma_b)}}. \quad (5)$$

Setting $V_{b,0} \sim r_0^3$ (i.e., initial bubble size is comparable with the initial distance from the cluster center) and $V_0 \sim R_0^3$, we get

$$r_{max} \sim r_0\left(\beta_0\frac{r_0}{R_0}\right)^{\frac{1}{2+\alpha-\alpha/\gamma-\alpha/\gamma_b}} \quad (6)$$

$$\beta(r_{max}) \sim \beta_0\left(\beta_0\frac{r_0}{R_0}\right)^{-\frac{2\gamma+\alpha(\gamma-2)}{2\gamma+\alpha(\gamma-1-\gamma/\gamma_b)}}\frac{R_0^2}{r_0^2}. \quad (7)$$

For a set of fiducial values $\alpha \sim 0.85$, $\gamma = 5/3$, $\gamma_b = 4/3$, $\beta_0 \sim 100$, we get

$$r_{max} = 10\ r_0\left(\frac{r_0}{R_0}\right)^{0.6} \quad (8)$$

$$\beta(r_{max}) \sim \left(\frac{r_0}{R_0}\right)^{-3}. \quad (9)$$

Thus, it is reasonable to expect the bubble to rise a distance of order $r \sim 10\ r_0$ before the buoyancy and magnetic forces come into balance. At this point, the β parameter in the stretched fluid elements approaches unity. Circumstantial evidence for the magnetic field energy density comparable to the ICM thermal pressure was indeed presented (based on a different argument) in Fabian et al. (2011); Werner et al. (2012).

4 RECONNECTION IN THE FILAMENTS

Once the bubble is at r_{max}, further stretching of the field lines is not possible. The bubble (or fluid elements attached to it) would "hang" on the magnetic field lines. However, the field lines in the stretched fluid elements will have opposite directions and are forced together by the shrinking cross section of the filament. The configuration bears strong similarity to the solar coronal loops (e.g., Kopp & Pneuman 1976) or the Earth magneto-tail (e.g., Nishida 2000), making the filament prone to reconnection. As the anti-parallel field lines come together, current sheets are formed, with an inflow of magnetic energy, which is eventually dissipated there. The release of magnetic energy allows the bubble to rise further.

Magnetic reconnection in both collisional (MHD) and collisionless plasmas proceeds at a rate that is independent of Ohmic resistivity (Uzdensky, Loureiro, & Schekochihin 2010) or other aspects of plasma microphysics (Rogers et al. 2001). Namely, one can write a rough estimate of the magnetic energy inflow per unit surface of the reconnecting layer as follows:

$$L_{rec} \approx \epsilon v_A\frac{B^2}{8\pi}, \quad (10)$$

where $v_A = \sqrt{\frac{B^2}{4\pi n \mu m_p}}$ is the Alfven speed, n is the gas particle density, μ mean particle atomic weight and ϵ is a dimensionless coefficient varying between $\epsilon \sim 0.01$ for collisional plasmas (Uzdensky, Loureiro, & Schekochihin 2010; Loureiro et al. 2012; Bhattacharjee et al. 2009; Daughton et al. 2009; Loureiro et al. 2009) and $\epsilon \sim 0.1$ for collisionless ones (Birn et al. 2001). Assuming that $\beta \sim 1$, we can replace the magnetic energy density with the thermal energy density $\frac{B^2}{8\pi} \sim nkT$ and the Alfven velocity v_A with the sound speed $c_s = \sqrt{\gamma \frac{P_{gas}}{\mu m_p}}$. This gives an order-of-magnitude estimate of the surface influx of energy[1]:

$$L_{rec} \approx \epsilon c_s nkT. \quad (11)$$

For the NGC1275 and M87 the estimates of the total emitted surface flux by the filaments are available (Fabian et al. 2011; Werner et al. 2012): $L_{em} \sim 10^{-2}$ ergs s^{-1} cm^{-2} $\sim 0.2 c_s nkT$ and $\sim$ 2.2 10^{-3} ergs s^{-1} cm^{-2} $\sim 0.1 c_s nkT$, respectively. Thus, there is an interesting order-of-magnitude agreement between the amount of energy that can be produced by fast reconnection and the amount of energy emitted by the filaments, i.e. $\frac{L_{rec}}{L_{em}} \approx \frac{\epsilon}{0.1}$. If the reconnection rate is on the stronger side of the possible values, viz. $\epsilon \sim 0.1$, the energy release from reconnection is comparable to the cooling losses of the filaments.

5 DISCUSSION

The overall energetics of the cool cores are believed to be determined by the balance of the AGN activity and gas cooling. In other words, one can assume that the cooling losses are approximately matched by the amount of mechanical energy pumped by the AGN into the gas in the form of relativistic bubbles. Observations suggest that a significant (if not dominant) fraction of the AGN energy goes into the enthalpy of the bubbles rather than in the shocks (e.g., Churazov et al. 2002). This means that potential energy of underdense bubbles created by the AGN per unit time approximately matches gas cooling losses. The estimates in §3 suggest that by the time when β reaches 1, the bubble has moved to $r_{max} \sim 10 r_0$. Let us estimate the ratio f_B of the magnetic energy of the stretched fluid element at this moment to the initial enthalpy of the bubble $H_0 = \frac{\gamma_b}{\gamma_b - 1} P_0 V_{b,0}$:

$$f_B = \frac{E_B}{H_0} \sim \frac{\gamma_b - 1}{\gamma_b} \frac{1}{\beta(r_{max})} \frac{PV}{P_0 V_{b,0}} \sim$$
$$\frac{\gamma_b - 1}{\gamma_b} \frac{1}{\beta(r_{max})} \left(\frac{r_{max}}{r_0}\right)^{-\alpha \frac{\gamma_b - 1}{\gamma_b}} \left(\frac{R_0}{r_0}\right)^3 \sim 0.1, \quad (12)$$

using eq.(3,7,8) and neglecting dependence on R_0/r_0. At r_{max}, the fraction of the remaining enthalpy of the bubble is

$$f_H = \frac{H}{H_0} = \frac{PV_b}{P_0 V_{b,0}} \sim \left(\frac{r_{max}}{r_0}\right)^{-\alpha \frac{\gamma_b - 1}{\gamma_b}} \sim 0.5. \quad (13)$$

The rest of the initial enthalpy has already been transferred to the gas via hydrodynamic drag, potential energy of the uplifted gas, magnetic energy, excitation of g-modes, which then dissipate in the ICM (Churazov et al. 2002). Comparison of f_H and f_B suggests that by the time the bubble reaches r_{max}, about 20% of its available energy will have gone into magnetic energy forced into its tail. The luminosity of the filaments from NIR to optical bands amounts to 10-20% of the bolometric luminosity of the cluster cores. This means that 10-20% of the potential energy available conversion into magnetic energy should indeed go into reconnection and the associated heating. When the reconnection releases magnetic energy, the bubble continues to rise beyond r_{max}. The partitioning of the remaining energy depends on the configuration, but it is likely to stay at the same level.

Note that it very likely that in real clusters there is a considerable spread in the values of initial parameters, such as, e.g., β_0, r_0/R_0. This suggests a large spread in the appearance of the filaments in different clusters or even of filaments/bubbles in the same cluster.

In our simple scenario, only the regions where the configuration of magnetic field is favorable for reconnection are observed as filaments. The energy of the magnetic field is the principal source of energy for the outer filaments, rather than ICM thermal energy or photoionization, although both can contribute. The implication is that the filaments do not necessarily grow in mass with time, instead they thermalize and emit the bubble energy, mediated by magnetic fields.

The cooling of the gas is not the central element of our model (cf. Soker & Sarazin 1990; Jafelice & Friaca 1996), in the sense that the main driver of the reconnection is the stretching of the field lines by the bubbles, rather then the loss of thermal energy by the cooling gas. It is nevertheless clear that a large amount of cool gas is present in these systems. In the simplest scenario, this gas intercepts, thermalizes and re-emits the released energy of the magnetic field. The discussion of how the magnetic energy is split between thee kinetic energy of the gas, its thermal energy and non-thermal particles, and of actual excitation of the optical lines is beyond the scope of this letter. We nevertheless note that the presence of non-thermal particles may help explain many properties of the emission spectra (Ferland et al. 2009).

As a speculative extension of this qualitative model, we note that the gas leaving the reconnection region will have

[1] Note that while the dissipation rate of the magnetic energy in the reconnection process does not have to be the same as the reconnection rate, it is reasonable to expect that they are comparable (there is some numerical evidence in support of this, e.g., Loureiro et al. 2012). In our simple estimates we have absorbed both the reconnection and the dissipation rate into the ϵ parameter.

velocities of order v_A, which is also of the order of the sound speed. The outflow is typically bi-directional, i.e., along the filaments. Reconnection in extended current sheets is typically accompanied by generation and ejection of copious number of plasmoids (Loureiro et al. 2012; Bhattacharjee et al. 2009; Daughton et al. 2009; Samtaney et al. 2009), some of them very large (Loureiro et al. 2012). If the filament is aligned along the line of sight towards an observer, this may lead to the appearance of gas lumps moving towards the core, away from the observer with a speed that can be as large as $\sim 10^3$ km s^{-1} for the hot gas. There is a so-called High Velocity system (HV) in the core of the Perseus cluster – a line emitting region in the core of NGC1275, with the recession velocity ∼3000 km/s larger than the systemic velocity of NGC1275 (e.g., Minkowski 1957), which is is nevertheless located in front of NGC1275 (e.g., De Young, Roberts, & Saslaw 1973) and therefore is moving towards the nucleus. While the infalling velocity of HV seems to be too large for a conceivable plasmoid-ejection mechanism, it is nevertheless interesting to note that in some favourable configurations, high-velocity gas lumps can be observed.

6 CONCLUSIONS

We argue that buoyant bubbles in the cores of galaxy clusters stretch the fluid elements advected from the core, forming gaseous filaments and aligning and amplifying the magnetic field in these filaments. The field grows to $\beta \sim 1$ after the bubbles rise a distance of order 10 times their size. The field lines in the wake of the bubble are anti-parallel and are forced together. This setup bears strong similarity to the coronal loops on the Sun or the Earth magneto-tail. The reconnection process can naturally explain both the required level of local dissipation rate in filaments and overall energy balance. In this model, the ultimate source of power for the filaments is the potential energy of buoyant bubbles, inflated by the central AGN. Of order 10% of the total mechanical energy deposited by the AGN in the form of relativistic bubbles can be converted into the emission from the filaments.

7 ACKNOWLEDGMENTS

EC acknowledges useful discussions with A.Petrukovich and H.Spruit. This work was supported in part by the Leverhulme Trust Network on Magnetized Plasma Turbulence. MR acknowledges NSF grant AST 1008454 and NASA ATP grant 12-ATP12-0017.

REFERENCES

Bhattacharjee A., Huang Y.-M., Yang H., Rogers B., 2009, PhPl, 16, 112102
Birn J., et al., 2001, JGR, 106, 3715
Boehringer H., Fabian A. C., 1989, MNRAS, 237, 1147
Carilli C. L., Taylor G. B., 2002, ARA&A, 40, 319
Churazov E., Forman W., Jones C., Böhringer H., 2000, A&A, 356, 788
Churazov E., Brüggen M., Kaiser C. R., Böhringer H., Forman W., 2001, ApJ, 554, 261
Churazov E., Sunyaev R., Forman W., Böhringer H., 2002, MNRAS, 332, 729
Churazov E., Forman W., Jones C., Böhringer H., 2003, ApJ, 590, 225
Conselice C. J., Gallagher J. S., III, Wyse R. F. G., 2001, AJ, 122, 2281
Daughton W., Roytershteyn V., Albright B. J., Karimabadi H., Yin L., Bowers K. J., 2009, PhRvL, 103, 065004
David L. P., Bregman J. N., Seab C. G., 1988, ApJ, 329, 66
De Young D. S., Roberts M. S., Saslaw W. C., 1973, ApJ, 185, 809
Fabian A. C., Sanders J. S., Crawford C. S., Conselice C. J., Gallagher J. S., Wyse R. F. G., 2003, MNRAS, 344, L48
Fabian A. C., Johnstone R. M., Sanders J. S., Conselice C. J., Crawford C. S., Gallagher J. S., III, Zweibel E., 2008, Natur, 454, 968
Fabian A. C., Sanders J. S., Williams R. J. R., Lazarian A., Ferland G. J., Johnstone R. M., 2011, MNRAS, 417, 172
Falceta-Gonçalves D., de Gouveia Dal Pino E. M., Gallagher J. S., Lazarian A., 2010, ApJ, 708, L57
Ferland G. J., Fabian A. C., Hatch N. A., Johnstone R. M., Porter R. L., van Hoof P. A. M., Williams R. J. R., 2009, MNRAS, 392, 1475
Forman W., et al., 2007, ApJ, 665, 1057
Forman W., et al., 2013, in preparation
Heckman T. M., Baum S. A., van Breugel W. J. M., McCarthy P., 1989, ApJ, 338, 48
Jafelice L. C., Friaca A. C. S., 1996, MNRAS, 280, 438
Kopp R. A., Pneuman G. W., 1976, SoPh, 50, 85
Lazareff B., Castets A., Kim D.-W., Jura M., 1989, ApJ, 336, L13
Loureiro N. F., Samtaney R., Schekochihin A. A., Uzdensky D. A., 2012, PhPl, 19, 042303
Loureiro N. F., Uzdensky D. A., Schekochihin A. A., Cowley S. C., Yousef T. A., 2009, MNRAS, 399, L146
Lynds R., 1970, ApJ, 159, L151
McDonald M., Veilleux S., Rupke D. S. N., Mushotzky R., 2010, ApJ, 721, 1262
Minkowski R., 1957, IAUS, 4, 107
Mittal R., et al., 2012, MNRAS, 426, 2957
Nishida A., 2000, SSRv, 91, 507
O'Neill S. M., De Young D. S., Jones T. W., 2009, ApJ, 694, 1317
Owen F. N., Eilek J. A., Kassim N. E., 2000, ApJ, 543, 611
Rogers B. N., Denton R. E., Drake J. F., Shay M. A., 2001, PhRvL, 87, 195004
Rubin V. C., Oort J. H., Ford W. K., Jr., Peterson C. J., 1977, ApJ, 211, 693
Ruszkowski M., Enßlin T. A., Brüggen M., Heinz S., Pfrommer C., 2007, MNRAS, 378, 662
Ruszkowski M., Enßlin T. A., Brüggen M., Begelman M. C., Churazov E., 2008, MNRAS, 383, 1359
Salomé P., et al., 2006, A&A, 454, 437
Samtaney R., Loureiro N. F., Uzdensky D. A., Schekochihin A. A., Cowley S. C., 2009, PhRvL, 103, 105004

Soker N., Sarazin C. L., 1990, ApJ, 348, 73
Spruit H. C., 2013, arXiv, arXiv:1301.5572
Uzdensky D. A., Loureiro N. F., Schekochihin A. A., 2010, PhRvL, 105, 235002
Voit G. M., Donahue M., Slavin J. D., 1994, ApJS, 95, 87
Werner N., et al., 2012, arXiv, arXiv:1211.6722